Combination rules for Structures under Bidirectional Horizontal Seismic Excitations: A Statistical Assessment of Responses

Reglas de Combinación para Estructuras bajo Excitaciones Sísmicas Horizontales Bidireccionales: Un Cálculo Estadístico de Respuestas

Adrian Pozos-Estrada[1], H.P. Hong[2], A. David García-Soto[3]

Recibido: Mayo 2025
Aceptado: Junio 2025
Publicado: Diciembre 2025

Palabras Clave:
Sismos; Movimiento del terreno; Diseño Sísmico; Efectos Sísmicos; Respuesta Estructural.

Keywords:
Earthquakes; Ground motion; Seismic design; Seismic effects; Structural response

RESUMEN

En ingeniería sísmica, el conjunto de ejes principales de las excitaciones sísmicas es definido con base en el tensor de la intensidad de Arias. Los ejes principales son empleados en la caracterización de las excitaciones sísmicas y con frecuencia interpretados como si las orientaciones de estos ejes representaran los ejes de la seudo-aceleración (SA) espectral máxima, intermedia y mínima. La interpretación de los ejes principales fue adoptada en la literatura para el desarrollo de la regla de combinación cuadrática completa extendida (CQC por sus siglas en inglés) para evaluar las respuestas estructurales bajo excitaciones sísmicas ortogonales multicomponentes y usada para seleccionar el ángulo crítico de incidencia sísmica. Sin embargo, el eje asociado con la SA máxima con frecuencia no coincide con el eje principal mayor y, depende del periodo natural de vibrar. Las implicaciones de lo anterior en la regla de combinación extendida CQC es desconocido. Asimismo, no hay una guía de cómo seleccionar la magnitud del espectro de respuesta para las dos direcciones horizontales ortogonales que serán usadas con la regla de la combinación extendida CQC. Lo anterior motivo a los autores para investigar la precisión de esta regla, la regla de la raíz cuadrada de la suma de los cuadrados y las reglas de porcentaje para estimar las respuestas bajo excitaciones sísmicas horizontales bidireccionales, y su uso junto con espectros de peligro uniforme o espectro de respuesta de diseño. Para la investigación, un conjunto de cerca de 600 registros reales del movimiento del terreno es empleado. El análisis de los resultados provee las bases para recomendaciones específicas en cómo definir los espectros para dos direcciones horizontales ortogonales y cómo corregir las desviaciones de estas reglas.

ABSTRACT

In seismic engineering, the set of orthogonal principal axes of seismic excitations is defined based on the Arias intensity tensor. The principal axes are then employed in characterizing the seismic excitations and often interpreted as if the orientations of these axes represent the axes of the maximum, intermediate and minimum pseudo-spectral acceleration (PSA) responses. This interpretation of the principal axes is adopted in developing the extended complete quadratic combination (CQC) rule in the literature for evaluating the responses of structures under multi-component orthogonal seismic excitations and used to select the critical angle of seismic incidence. However, the axis associated with the maximum PSA response often does not coincide with the major principal axis and, depends on the natural vibration period. The implication of this on the extended CQC rule is unknown. Furthermore, there is no guideline on how to select the magnitude of the response spectra for the two orthogonal horizontal directions that are to be used with the extended CQC rule. These motivated us to investigate the accuracy of this rule, the square-root-of-sum-of-squares rule and the percentage rules for estimating the responses under bidirectional horizontal seismic excitations, and their use together with uniform hazard spectra or design response spectrum. For the investigation, a set of about 600 actual strong ground motion records is employed. The analysis results provided the basis for specific recommendations on how to define the spectra for two orthogonal horizontal directions and how to correct the biases in these rules.

*Autor para correspondencia. Adrián Pozos Estrada
Direccion de correo electrónico: apozose@iingen.unam.mx

1 1Institute of Engineering, National Autonomous University of Mexico, Mexico D.F.

2 Department of Civil and Environmental Engineering, University of Western Ontario, Canada N6A 5B9

3 Department de Ingeniería Civil, Universidad de Guanajuato, Campus Guanajuato, Sede Belén, Avenue Juárez 77, Zona Centro, C.P. 36000 Guanajuato, Mexico

1. INTRODUCCIÓN

Structures are subjected to multicomponent seismic excitations. One is often interested in the structural responses to the orthogonal horizontal strong ground motions. To characterize the orthogonal horizontal ground excitations, the Arias intensity tensor has been employed in defining the principal axes of ground excitations along which the ground excitations are considered to be uncorrelated (Arias 1970, 1996, Penzien and Watabe 1975, Kubo and Penzien 1979). It seems that the major, intermediate, and minor principal axes are taken to be as if they represented the axes with the major, intermediate, and minor responses for selecting the critical angle of seismic incidence (Smeby and Der Kiureghian 1985, Menun and Der Kiureghian 1998, Lopez et al. 2001, Anastassiadis et al. 2002). However, recent findings showed that the axis associated with the maximum pseudo-spectral acceleration (PSA) response often does not coincide with the major principal axis and, depends on the natural vibration period (Hong and Goda 2007, Pozos-Estrada et al. 2007). Therefore, the seismic excitation model based on the principal axes, that was adopted for developing the extended complete quadratic combination (CQC) rule for structures under multicomponent excitations (Smeby and Der Kiureghian 1985), and the accuracy of the extended CQC rule should be verified or validated using sufficient number of actual strong ground motion records. For structural systems with significant torsional effects, mass eccentricity, or closely spaced modes, the CQC3 rule is generally preferred as it can handle closely spaced modes and modal correlation, including torsional coupling.

The validation of the CQC rule can only be carried out in statistical sense since the seismic excitations including the incidence angle are uncertain. Furthermore, to the authors' knowledge, there is no guideline on how to select the response spectra for the two orthogonal horizontal directions if the uniform hazard spectra (UHS) or the design spectrum for randomly oriented single-degree-of-freedom systems are given.

It is worth mentioning that for more complex structural systems (e.g., those with modal and torsional interaction), some studies have shown that current seismic design codes have conflicts on whether the orthogonal seismic effects should be considered for torsionally irregular structures (Wang et al., 2024). Other studies have evaluated percentage combination rules considering the collapse performance of special concentrically braced frames (Wang et al., 2021).

The objective of the present study is to carry out a statistical assessment of the peak response of structures under two orthogonal horizontal ground excitations; to assess the accuracy of the extended CQC rule (Smeby and Der Kiureghian 1985), the square-root-of-sum-of-squares (SRSS) rule, the 40% rule (Newmark 1975) and the 30% rule (Rosenblueth and Contreras 1977); and to provide recommendations for selecting the response spectra in two orthogonal horizontal directions that are to be used in conjunction with the SRSS rule and the extended CQC rule. To facilitate the discussions and the assessment of the rules, the basic assumptions leading to the rules, especially for the extended CQC rule, are summarized in the following section. For the assessment, sets of observed strong ground motion records are employed, and the implications of the results in codified design are highlighted. Since the number of the combinations of the parameters describing the structures can be extremely large for carrying out a comprehensive assessment of the rules, the analyses in the present study are concentrated only on single storey symmetric structures under orthogonal horizontal ground excitations.

2.DISCUSSIONS OF THE EXTENDED COMPLETE QUADRATIC COMBINATION RULE FOR MULTICOMPONENT SEISMIC EXCITATIONS

The information on the development and the usefulness of the complete quadratic combination (CQC) rule for estimating the peak structural responses under seismic excitations have been given by Der Kiurehgian (1981) and Chopra (2001). The satisfactoriness of the use of the CQC rule together with the uniform hazard spectrum (UHS) has been assessed based on reliability analysis and random vibration theory (Hong and Wang 2002, Wang and Hong 2005). The extension of the CQC rule for estimating the peak response of structures under multicomponent excitations was developed by Smeby and Der Kiureghian (1985). To facilitate the discussion and verification of the rule, the basic assumptions and the adopted seismic ground motion model used for developing the rule are summarized in the following.

Consider that a structure under mutlticomponent excitations can be modeled as a linear elastic multi-degree-of-freedom (MDOF) system. A response of interest of the structure, R(t), can be expressed as a

combination of the nodal displacements denoted by U which can be obtained by solving the following equation of motion,

$$\mathbf{M}\ddot{\mathbf{U}} + \mathbf{C}\dot{\mathbf{U}} + \mathbf{K}\mathbf{U} = -\mathbf{M}\mathbf{I}\ddot{\mathbf{U}}_g \qquad (1)$$

where **M**, **C**, and **K** are the mass, damping and stiffness matrices; is the vector of nodal displacement; dots indicate the time derivatives; **I** is an influence matrix and $\ddot{\mathbf{U}}_g$ is the vector of no more than three translational ground excitations.

Since the seismic excitations are stochastic processes, R(t) is also a stochastic process and its mean peak response is related to its power spectral density function. To simplify the analysis and to provide a simple to use equation to estimate the mean peak response of R(t), μ_R, Smeby and Der Kiureghian (1985) considered the observations made by Penzien and Watabe (1975) (see also Arias 1970), indicating that there exists a set of orthogonal principal axes of the ground excitations along which the ground excitations are uncorrelated, and that one of the principal axis is almost always vertical. Based on this adopted excitation model, the random vibration theory, and considering that the peak factors (i.e., ratio of the mean to the standard deviation of the peak response) for each vibration mode as well as for the response of interest R(t) are approximately equal, it was concluded that the mean peak response of R(t), μR, can be estimated from,

$$\mu_R = \left(\sum_{k=1}^{3}\sum_{i=1}^{n}\sum_{j=1}^{n} C_{i,k}C_{j,k}\rho_{ij}\mu_{i,k}\mu_{j,k} - \sin^2\theta \sum_{i=1}^{n}\sum_{j=1}^{n}\left(C_{i,1}C_{j,1} - C_{i,2}C_{j,2}\right)\rho_{ij}\left(\mu_{i,1}\mu_{j,1} - \mu_{i,2}\mu_{j,2}\right) - \sin 2\theta \sum_{i=1}^{n}\sum_{j=1}^{n} C_{i,1}C_{j,2}\rho_{ij}\left(\mu_{i,1}\mu_{j,1} - \mu_{i,2}\mu_{j,2}\right) \right)^{1/2} \qquad (2)$$

where *n* is the total number of vibration modes, $C_{i,k}$ is the effective participation factor of *i*-th mode associated with *k*-th component of ground motion, $\mu_{i,k}$ denotes the mean peak modal response for the i-th mode with *k*-th component of ground motion in which *k* = 3 represents the vertical component, ρ_{ij} is the modal correlation coefficient of the responses between the *i*-th and *j*-th modes (Der Kiureghian 1981), and θ is the angle between the set of structural principal axes and the set of principal axes in the horizontal plane.

Eq. (2) is referred to as the CQC3 rule by Menun and Der Kiureghian (1998). In arriving at these conclusions, Smeby and Der Kiureghian (1985) stressed that this equation is specific to the adopted seismic ground excitation model – the existence of the orthogonal principal axes of the ground excitations and identical spectral shape. However, it has been observed that (Hong and Goda, 2007; Pozos-Estrada et al. 2007):

1) The axis along which the peak response of a single-degree-of-freedom (SDOF) system is maximum (i.e., major response axis) does not coincide with the major principal axis; and

2) The ratio of the peak response for a SDOF with an arbitrary orientation to the maximum peak response (i.e., maximum resultant response) for a record in the horizontal plane cannot be adequately represented by an ellipsoid. Strictly speaking, this is true even by averaging the ratios obtained from many records. The average is natural vibration period dependent.

The above observations are illustrated in Figure 1 for an arbitrarily selected record. The first observation can be explained by noting that the principal axis is defined based on the Arias intensity which is a measure of the sum of the distributed energy in a range of frequencies whereas the maximum peak response is sensitive to the energy of the excitations associated with a particular frequency. Therefore, the orientation of the major principal axis does not represent the major response axis. The second observation simply reflects that the peak response is sensitive to energy distribution (of the nonstationary process) in time and frequency domain, and that the adequacy or accuracy of the extended CQC rule which is based on the assumption of identical spectral shape for the two principal horizontal axes needs to be validated. In other words, there is a need for assessing or validating the rule using the actual strong ground motion records. The need for such an assessment is further justified by noting that many studies (Menun and Der Kiureghian 1998, 2000, Lopez et al. 2001, Anastssiadis et al. 2002) use the predicted responses from the extended CQC rule as the benchmark to select the critical excitation orientation, and to assess the accuracy of the approximate combination rules such as the SRSS rule and, the percentage rules.

An aspect relating to the CQC rule which needs to be emphasized is that Eq. (2) is derived for esti-

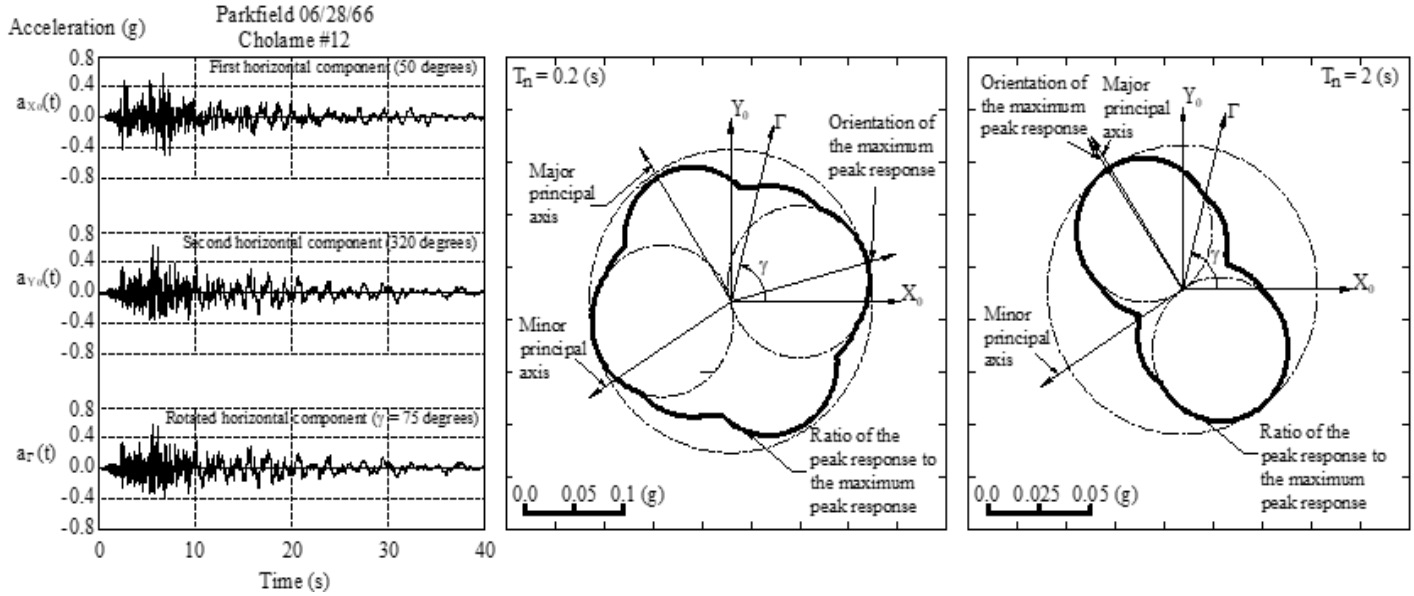

Figure 1. Illustration of response axes, principal axes and orientation effects on the records and the PSA.

mating the mean peak response rather than the peak response for a specified exceedance probability level. It is shown that the accuracy of the CQC rule for estimating the fractile of peak response is similar to that for estimating the mean peak response for structures under a single component of horizontal ground excitations (Hong and Wang 2002, Wang and Hong 2005). However, whether this conclusion is valid for structures under multicomponent seismic excitations is unknown, although it is implied that the extended CQC rule could be used in estimating the fractiles of peak response in some applications. With this observation, one could consider that Eq. (2) can be use to relate the peak response of R(*t*), rc, to the peak modal responses, $r_{i,k}$, for the same given probability level by replacing μ_R and $\mu_{i,k}$ with r_c and $r_{i,k}$, respectively, where $r_{i,k}$ represents the peak modal response (with the effective participation factor equal to one) for the *i*-th mode with *k*-th component of ground motion.

In particular, if the spectral shape for the two horizontal axes are the same (i.e., $r_{i,2}= \gamma \times r_{i,1}$) and the vertical component is ignored, Eq. (2) reduces to (Menun and Der Kiureghian 1998),

$$r_c = \left(R_1^2 + R_2^2 - \left(1-\gamma^2\right)\left(R_1^2 - \frac{1}{\gamma^2} R_2^2 \right) \sin^2\theta + \left(\frac{1-\gamma^2}{\gamma} \right) R_{12} \sin 2\theta \right)^{1/2} \qquad (3a)$$

where $R_k^2 = \sum_{i=1}^{\cdot\cdot} \sum_{j=1}^{\cdot\cdot} C_{i,k} C_{j,k} \rho_{ij} r_{i,k} r_{j,k}$ and

$R_{kl} = \sum_{i=1}^{n} \sum_{j=1}^{n} C_{i,k} C_{j,l} \rho_{ij} r_{i,k} r_{j,l}$, and the critical angle of seismic incidence θ_{cr} is given by,

$$\theta_{cr} = \frac{1}{2} \tan^{-1}\left(\frac{2R_{12}/\gamma}{R_1^2 - R_2^2/\gamma^2} \right), \qquad (3b)$$

Note that the use of the uniform hazard spectra (UHS) is recommended in codified design (e.g., NBCC 2005) which is commonly developed based on the seismic source zone models, the earthquake occurrence modeling and the ground motion prediction equation (GMPE) (i.e., attenuation relations of the PSA) (Frankel et al. 1996, Adams and Atkinson 2003). The attenuation of the PSA used for evaluating the UHS is for a randomly oriented SDOF system rather than the maximum PSA among all possible orientations (Boore et al. 2006, Hong and Goda 2007). Therefore, the seismic design spectrum determined in such a manner does not represent the spectrum for any of the principal axes in the horizontal plane. In other words, the critical response for a structure under orthogonal horizontal ground motions, which is

calculated using the extended CQC rule and assuming identical spectral shape for the two principal horizontal axes, needs to be validated.

3. STRUCTURES AND STRONG GROUND MOTION RECORDS

The preceding sections indicate that the commonly available combination rules for estimating the responses under multicomponent seismic excitations are the extended CQC rule, the SRSS rule and the percentage rule. The SRSS rule and the percentage rules could be viewed as approximations to the CQC rule. However, none of these rules is exact. Therefore, an estimate of the response obtained by one of the rules may not be employed as a yardstick to measure the accuracy of the remaining rules.

It is noted that a comprehensive and systematical assessment of the rules requires the consideration of an extremely large number of the combinations of the effective participation factor, frequency and damping ratio of each mode, the actual ground motion records, the angle between the set of structural principal axes and the set of principal direction of excitations (or the recording sensors orientations). To simplify such a parametric analysis, this study considers only single storey symmetric buildings under two horizontal orthogonal excitations. Single storey buildings with unsymmetric plane or with mass eccentricity are not considered since they require the consideration of the modal combination analysis for the structure under a component of horizontal excitations along a structural principal axis, and thus creating difficulties in assessing whether any possible deficiencies of the rules are due to the effects of bidirectional excitations or the higher modes.

The idealized single storey building to be analyzed has a rigid slab as illustrated in Figure 2, and the equation of motion without considering damping effect is given by,

$$\begin{bmatrix} m & 0 \\ 0 & m \end{bmatrix} \begin{Bmatrix} \ddot{u}_x \\ \ddot{u}_y \end{Bmatrix} + \begin{bmatrix} k_x & 0 \\ 0 & k_y \end{bmatrix} \begin{Bmatrix} u_x \\ u_y \end{Bmatrix} = -\begin{Bmatrix} m\ddot{u}_{gx}(t) \\ m\ddot{u}_{gy}(t) \end{Bmatrix} \qquad (4)$$

where m is the lumped mass of the system; u_x and u_y denote the displacement in x- and y- directions respectively; $\ddot{u}_x$ and $\ddot{u}_y$ represent the second order time derivative of u_x and u_y.

To facilitate the parametric study and to take the damping effect into account, we consider that $\omega_x = \sqrt{k_x / m}$, $\eta_y = \omega_y / \omega_x$, η_y is a parameter used to normalized the damping matrix. This parameter is a dimensionless quantity that describes how the dynamic characteristics of two different vibration modes compare. Depending of the value of this parameter, one can inferred if the modes are closely spaced, and modal coupling is likely significant. This affects how modal combination rules should be applied.

$\omega_y = \sqrt{k_y / m}$; and that the classical damping matrix of the structure can be derived based on the modal damping coefficient leading to the modal damping ratio equal to ξx and ξy for the vibration along the x- and y- directions, respectively. This leads to that Eq. (5) can be re-written as,

$$\begin{Bmatrix} \ddot{u}_x \\ \ddot{u}_y \end{Bmatrix} + 2\omega_x \begin{bmatrix} \xi_x & 0 \\ 0 & \xi_y \eta_y \end{bmatrix} \begin{Bmatrix} \dot{u}_x \\ \dot{u}_y \end{Bmatrix} + \omega_x^2 \begin{bmatrix} 1 & 0 \\ 0 & \eta_y^2 \end{bmatrix} \begin{Bmatrix} u_x \\ u_y \end{Bmatrix} = -\begin{Bmatrix} \ddot{u}_{gx}(t) \\ \ddot{u}_{gy}(t) \end{Bmatrix} \qquad (5)$$

Through out this study, unless otherwise indicated, a modal damping ratio of 5% is considered for all the numerical analyses.

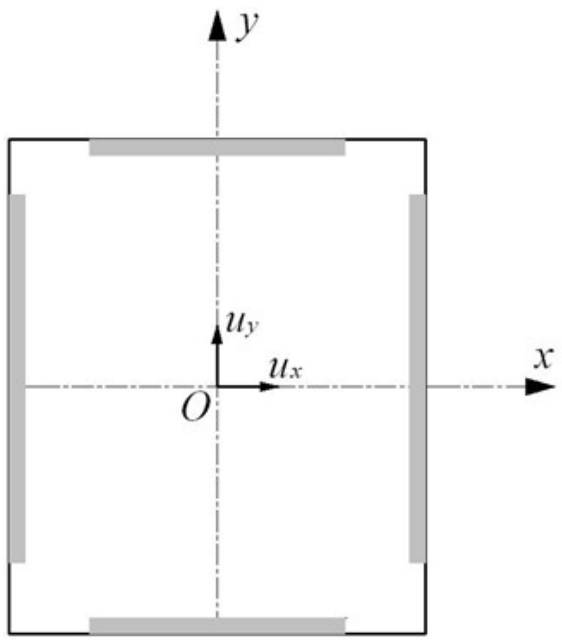

Figure 2.Schematic of plan of single-story symmetric system.

Given a record, Eq. (5) can be solved using the Newmark method, and the maximum of a response of interest, $R(t)$, r_{max}, can be calculated using the obtained response time history of the structure. Consequently, statistics of r_{max} can be obtained for a selected set of records. For the obtained statistics of r_{max} to be meaningful one must use a set of judiciously selected records.

It is noted that the criteria used to selected strong ground motion records to develop the attenuation relations, which take into account inhomogeneous tectonic regime, fault mechanism and data quality, are well documented (Abrahamson and Silva 1997, Boore et al. 1997, Steidl and Lee 2000, Campbell and Bozorgnia 2003). Based on these mentioned studies and an extensive set of strong ground motion records included in the NGA database for California earthquakes (PEER, 2006), Hong and Goda (2007) selected a set of 592 records from 39 earthquakes, which is employed in the present study; and estimated the coefficients of the following GMPE (i.e., attenuation relation) for the natural vibration period T_n ranging from 0.1 to 2 (s),

$$\ln Y = b_1 + b_2(M-7) + b_3(M-7)^2 + \left(b_4 + b_5(M-4.5)\right)\ln\left((d^2+h^2)^{0.5}\right) + AF_s + \varepsilon, \quad (6)$$

In Eq. (6), Y denotes the PSA at period Tn, expressed in units of gravity (g), for SDOF systems. Depending on the context, Y may refer either to A(Tn), the PSA for a randomly oriented SDOF system, or to A_{MAXR} (Tn), the maximum PSA obtained by rotating the horizontal components to identify the orientation that yields the peak response; b_i, i = 1,…,5, are the model parameters; M is the moment magnitude of the earthquake; d (km) is the closest horizontal distance from the station to a point on the Earth's surface that lies directly above the rupture and is taken equal to the Joyner and Boore distance or the epicentral distance when the former is not available; h (km) represents a fictitious depth; AFs represents the amplification factor due to linear and nonlinear soil behaviour; and ε denotes the sum the intra-event variability ε_r and the inter-event variability ε_e. Note that the parameter b_1 is defined for unspecified fault mechanisms. The adopted AFs is the one suggested by Atkinson and Boore (2006) and Boore and Atkinson (2006), which is a function of the shear wave velocity Vs and the (expected) peak ground acceleration at the reference soil condition PGA_{ref} for Vs equal to 760 m/s. The adopted relation to calculate the PGA_{ref} is given as,

$$\ln PGA_{ref} = b_1 + b_2(M-7) + b_4 \ln\left((d^2+h^2)^{0.5}\right) \quad (7)$$

where b_1, b_2 and b_4 are the model parameters. For easy reference a few set of model parameters for Eqs. (6) and (7) are illustrated in Table 1.

Table 1. Attenuation coefficients for the geometric mean (i.e., AGM(Tn)), and the reference peak ground acceleration (i.e., PGAref) (Hong and Goda 2007).

Ground motion measure	T_n (s)	b_1	b_2	b_3	b_4	b_5	h (km)	$\sigma_{\varepsilon e}$	$\sigma_{\varepsilon r}$	σ_{ε}
	0.2	2.171	0.305	-0.045	-1.158	0.061	8.0	0.156	0.475	0.534
$A(T_n)$	0.5	1.405	0.965	-0.001	-0.746	-0.073	5.7	0.214	0.526	0.608
	1.0	0.481	0.644	-0.229	-0.843	-0.002	4.9	0.326	0.559	0.694
$PGA_{ref,GM}$	-	0.851	0.480	-	-0.884	-	6.3	-	-	-

It must be emphasized that the GMPEs for $A(T\text{n})$ are often developed based on the geometric mean, $A_{GM}(T\text{n})$, with a correction to the standard deviation of the error term ε (Boore et al. 1997) and, used for developing the UHS (Frankel et al. 1996, Adams and Atkinson 2003). The relations developed based on $A_{MaxR}(T\text{n})$ represent the response for the SDOF systems oriented along critical angle of seismic incidence (Hong and Goda 2007).

The assessment of the mean of the ratios between $A(T\text{n})$ and $A_{MaxR}(T\text{n})$, between $A(T\text{n})$ and the PSA for the minor response axis $A_{MinR}(T\text{n})$, between $A(T\text{n})$ and the PSA for the major principal axis $A_{Pma}(T\text{n})$, and between $A(T\text{n})$ and the PSA for the minor principal axis $A_{Pmi}(T\text{n})$, are also carried out and the results are shown in Table 2 for a few selected vibration periods. The table indicates that the means of the ratios $A_{MaxR}(T\text{n})/A(T\text{n})$, $A_{MinR}(T\text{n})/A(T\text{n})$, $A_{Pma}(T\text{n})/A(T\text{n})$, and $A_{Pmi}(T\text{n})/A(T\text{n})$ vary with vibration frequency. For convenience, if one is interested in using a single value for each ratio, one could consider 1.15 and 0.95 for the means of $A_{Pma}(T\text{n})/A(T\text{n})$, and $A_{Pmi}(T\text{n})/A(T\text{n})$ and, 1.30 and 0.70 for the means of $A_{Pma}(T\text{n})/A(T\text{n})$, and $A_{Pmi}(T\text{n})/A(T\text{n})$.

4. STATISTICAL ASSESSMENT OF RESPONSES UNDER BIDIRECTIONAL SEISMIC EXCITATIONS

4.1 Characteristics of the responses

To characterize the structural response under bidirectional excitations as a function of earthquake magnitude and distance, consider that the structure is under bidirectional excitations with governing equation shown in Eq. (5), and that the response of interest $R(t)$ can be expressed as,

$$R(t) = C_x u_x + C_y u_y = C_y\left(\zeta_x u_x + u_y\right) \qquad (8)$$

where C_x and C_y are the coefficients relating the displacements to the response of interest, and $\zeta_x = C_x/C_y$. For simplicity, C_y is set equal to one since it can be viewed as a normalization constant.

Consider that the structure is subjected to the excitations of an arbitrarily selected ground motion record shown in Figure 1. For the moment, it is considered that the structural principal axes coincide with the orientations of the recording sensors. The maximum of the absolute value of $R(t)$, r_{max}, obtained by solving Eqs. (5) and (8) is illustrated in Figure 3a for $\zeta x = 3$, $T_{nx} = 0.2$, and $\eta_y = 1$. Since the structural principal axes may not coincide with the orientations of the recording sensors, the evaluation of rmax is also carried out by varying the angle between the structural principal axes and the ground motion recording axes θ (i.e., rotate structure counterclockwise, or rotate the orientations of the recording sensors clockwise) and the results are also shown in Figure 3a. Note that there is periodicity of 180° in r_{max}. Similar analysis is carried out and the results are shown in Figure 3b but for $\zeta_x = 3$, $T_{nx} = 0.5$, and $\eta_y = 0.5$. The results shown in Figure 3 indicate that the maximum of r_{max}, denoted by $r_{max,c}$, occurs for different angles of seismic incidence

Table 2. Mean of the ratios of PSA for different axes.

Ratio	T_n (s)		
	0.2	0.5	1
$A_{MaxR}(T_n)/A(T_n)$	1.26	1.29	1.32
$A_{MinR}(T_n)/A(T_n)$	0.73	0.69	0.66
$A_{Pma}(T_n)/A(T_n)$	1.15	1.17	1.17
$A_{Pmi}(T_n)/A(T_n)$	0.93	0.93	0.95

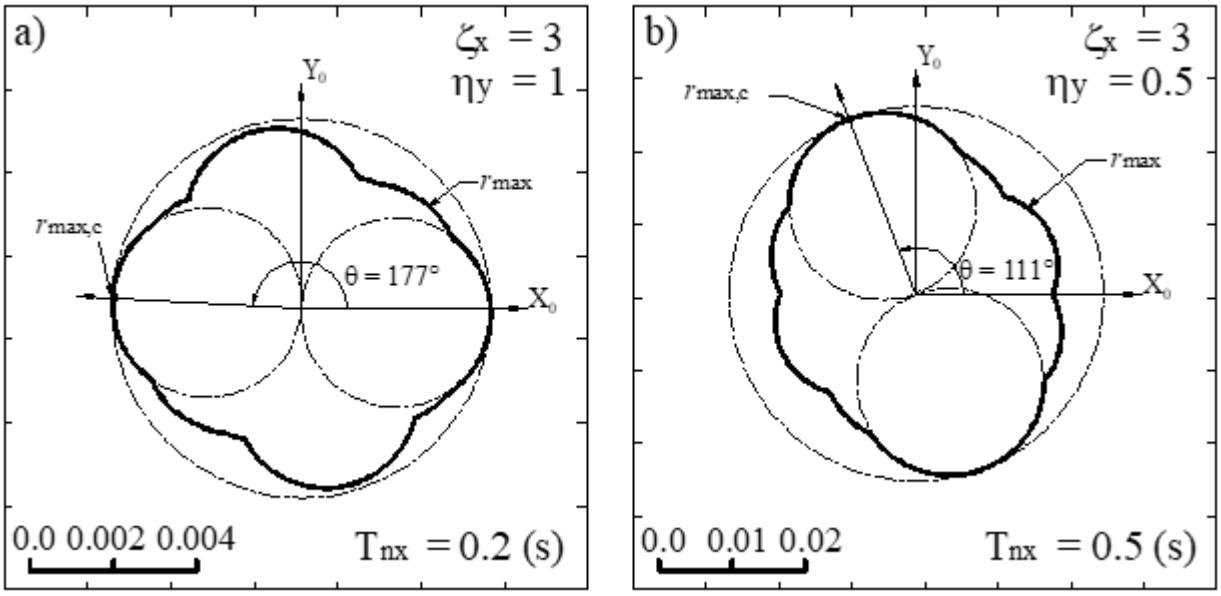

Figure 3.Illustration of the effect of angle of seismic incidence on the structural response considering bidirectional excitation.

for the two considered cases and, that the values of r_{max} in the horizontal plane does not resemble an ellipsoid. Further, the critical angle of seismic incidence does not coincide with the principal axes of the record.

Since the seismic loading is a stochastic process, to assess the statistical characteristics of r_{max} for all possible angles of seismic incidence, the values of r_{max} as well as the ratio $r_{max}/r_{max,c}$ are calculated for each of the 592 records mentioned earlier for $\zeta_x = 3$, $T_{nx} = 0.2$, and $\eta_y = 1$. These ratios are plotted in Figures 4a to 4c to identify possible trends. For the results shown in Figure 4a it is considered that the structural principal axes and the recording orientations initially coincide and then the axes of the seismic excitations are rotated clockwise. For the results shown in Figure 4b, it is considered that initially the structural principal axes and the recording orientations are placed in such a way that $r_{max,c}$ is attained. Finally, for results shown in Figure 4c, it is considered that the structural principal axes and the principal axes coincide initially and r_{max} is the greatest for all possible combinations of such coincidences.

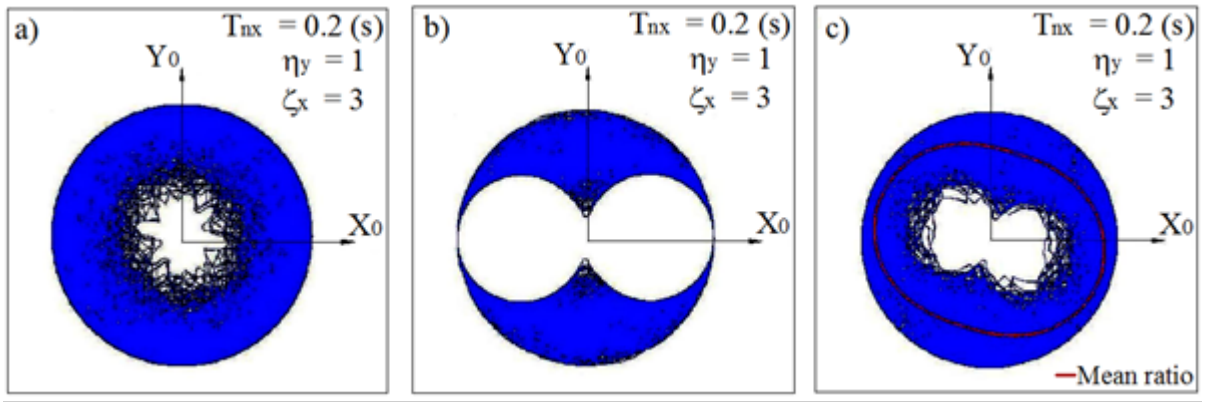

Figure 4.Effect of angle of seismic incidence on the normalized structural response (i.e., $r_{max}/r_{max,c}$) considering bidirectional excitation for $\zeta_x = 3$, $T_{nx} = 0.2$, and $\eta_y = 1$.

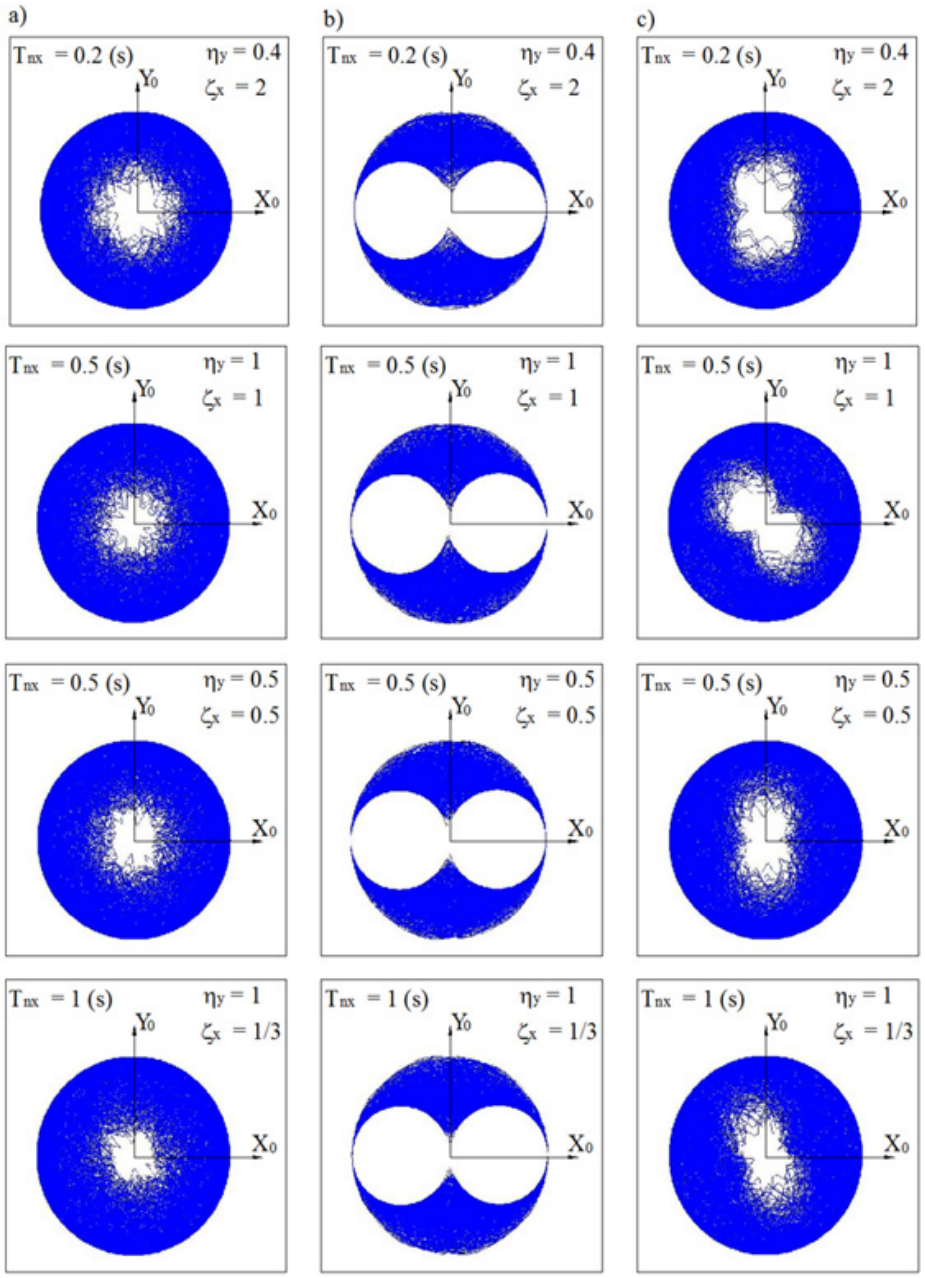

Figure 5.Effect of angle of seismic incidence on the normalized structural response (i.e., $r_{max}/r_{max,c}$) considering bidirectional excitation.

a) for $\zeta_x = 2$, $T_{nx} = 0.2$, and $\eta_y = 0.4$.

b) for $\zeta_x = 1$, $T_{nx} = 0.5$, and $\eta_y = 1$.

c) for $\zeta_x = 0.5$, $T_{nx} = 0.5$, and $\eta_y = 0.5$.

d) for $\zeta_x = 1/3$, $T_{nx} = 1$, and $\eta_y = 1$.

Figure 4a indicates that by considering the randomness in the recording orientations and the structural principal axes, the mean of the r_{max} (considering all possible structural principal axis orientations) is about 0.82 of $r_{max,c}$. As shown in Figure 4b, the ratio falls within a circle of radius 1.0 but almost always outside of two inner mutually exclusive small circles of radius 0.5, which is termed as the "goggle" phenomenon observed for the SDOF systems (Hong and Goda 2007). The mean of the ratio is about 0.67 along the Y_0-axis. The results shown in Figure 4c suggest that the mean of the ratio is about 0.73 along Y_0-axis, and 0.90 along X_0-axis. Also, the mean of the ratio conditioned on any given direction is plotted in Figure 4c to appreciate its variation and the angle of seismic incidence associated with the maximum of the mean of the ratio. The figure shows that the maximum of the mean of $r_{max}/r_{max,c}$ occurs at about 163°, and equals about 0.92. The results presented in Figure 4c further indicate that there is significant scatter on the obtained $r_{max}/r_{max,c}$ along any direction.

The above analysis is repeated for a few selected sets of values of ζ_x, ω_x and η_y (i.e., structures); the obtained results are shown in Figure 5. Comparison of the results shown in Figures 4 and 5 indicates that the conclusions drawn from Figure 4 are equally applicable to those shown in Figure 5, except that the mean values of the ratios differ slightly which is summarized in Table 3. The latter simply indicates that the mean of the ratio depends on the characteristics of the considered structure. In general, it can be concluded that r_{max} is, on average, about 81% of $r_{max,c}$.

Table 3. Mean of ratios for different structural parameters.

Structure characteristics			(1)	(2)	(3)	(4)	(5)
ζ_x	T_{nx}	η_y					
3	0.2	1	0.82	0.67	0.74	0.89	0.92
2	0.2	0.4	0.82	0.67	0.88	0.74	0.88
1	0.5	1	0.80	0.62	0.81	0.80	0.91
0.5	0.5	0.5	0.80	0.62	0.88	0.72	0.88
1/3	1	1	0.79	0.59	0.87	0.71	0.89

Note:(1) Mean of the ratio of rmax (considering all possible structural principal axis orientations) to $r_{max,c}$; (2) Mean of the ratio of r_{max} along Y_0-axis to $r_{max,c}$ from Figures 4b and 5b; (3) Mean of the ratio of r_{max} along Y_0-axis to $r_{max,c}$ from Figures 4c and 5c; (4) Mean of the ratio of r_{max} along X_0-axis to $r_{max,c}$ from Figures 4c and 5c; (5) The maximum of the mean of $r_{max}/r_{max,c}$ from Figures 4c and 5c.

4.2 Assessment of the combination rules

It is noted that the combination rules, namely, the extended CQC rule, the SRSS rule and the percentage rules, are often used for design purposes, and most recent design spectra are developed based on the GMPEs for $A(T\text{n})$. Consequently, it is of interest to assess the characteristics of the peak response of $R(t)$ defined in Eq. (8) using the combination rules and the predicted PSA values associated with principal directions. However, the design spectra or the PSA values suggested in the design codes represent the PSA for randomly oriented SDOF systems rather than those for the principal directions. Since this is likely to be the same at least in the near future, it is desirable to take this into account in the following assessment.

Note that for given structural characteristics (i.e., ζ_x, T_{nx}, and η_y), as shown in the previous section, one could calculate the rmax and rmax,c for each of the considered records whose earthquake magnitude and distance (M, d) are known. One could also calculate the peak response of $R(t)$, r_c, using one of the combination rules and the PSA values predicted by the GMPE for the same (M, d). Note that if the extended CQC rule is employed, one could also find the critical response r_{cr} (i.e., the maximum of r_c), using Eq. (3), and its corresponding critical angle of incidence θ_{cr}.

For the moment, consider that Eq. (6) for $A(T_n)$ can be used to predict the PSA for the two orthogonal horizontal orientations. This consideration is based on the observation that the GMPEs are employed to develop the UHS and design spectrum. To investigate the accuracy of the combination rules, an assessment of statistics of the ratio of the peak response obtained from time history under bidirectional excitations to the peak response predicted by the combination rules is carried out. More specifically, for each considered structure the assessment of the ratio is carried out by the following steps:

1) Evaluate r_{max}, for the i-th record (with corresponding magnitude and distance denoted by $(M, d)_i$) by considering that the structural principal axes coincide with the orientations of the recording sensors. This coincidence is selected randomly from one of the two possible such coincidences (note that since one is interested in the maximum of the absolute value of $R(t)$, the four possible coincidences reduce to two).

2) Calculate the peak response of $R(t)$ by using the SRSS, the 40% and 30% combinations rules, which are denoted by r_{srss}, $r_{40\%}$ and $r_{30\%}$ respectively, and by considering that the modal response along the structural principal axes can be predicted using the GMPE for $A(T\text{n})$ shown in Eq. (6) for $(M, d)_i$ and ε equal to zero. Note also that the extended CQC rule reduces to the SRSS rule under the above consideration, thus the results for the former and the latter are the same.

3) Calculate the ratio r_{max}/r_{rule} for the i-th record, where the subscript "rule" denotes SRSS, 40% and 30%.

4) Repeat Steps 1) to 3) for all the considered records.

The calculated ratios are plotted versus the magnitude M, distance d and r_{srss} in Figure 6 for the structure shown in Figure 4. The results presented in Figure 6 suggest that the logarithmic of the ratios could be assumed to be linearly uncorrelated with M, d and $\ln(r_{srss})$. Similar plots suggest that the same is true for structures shown in Figure 5, and for that reason they are not presented. Furthermore, plots of r_{max}/r_{rule} versus M, d and r_{srss} are carried out, and the results shown again that the former could be assumed to be linearly uncorrelated to the latter.

$$\ln\left(r_{\max} / r_{rule}\right) = a + \eta \qquad (9a)$$

$$\ln\left(r_{\max}\right) = \ln\left(r_{rule}\right) + a + \eta \qquad (9b)$$

where a is a regression coefficient, η equals $\eta_e + \eta_r$ in which η_e represents the inter-event variability with zero mean and ηr represent the intra-event variability with zero mean. For the case presented in Figure 6, the obtained a, the standard deviation of η_r, $\sigma_{\eta r}$, and the standard deviation of η_e, $\sigma_{\eta e}$, through regression analysis are shown in Table 4. The results presented in the table indicate that for this particular case the obtained variability $\sigma_{\eta r}$ and $\sigma_{\eta e}$ are similar to $\sigma_{\eta r}$ and $\sigma_{\eta e}$ shown in Table 1; and that the bias is about -1% (i.e., exp(-0.011)-1) for the SRSS rule, -8% (i.e., exp(-0.084)-1) for the 40% rule and the -5% (i.e., exp(-0.054)-1) for the 30% rule.

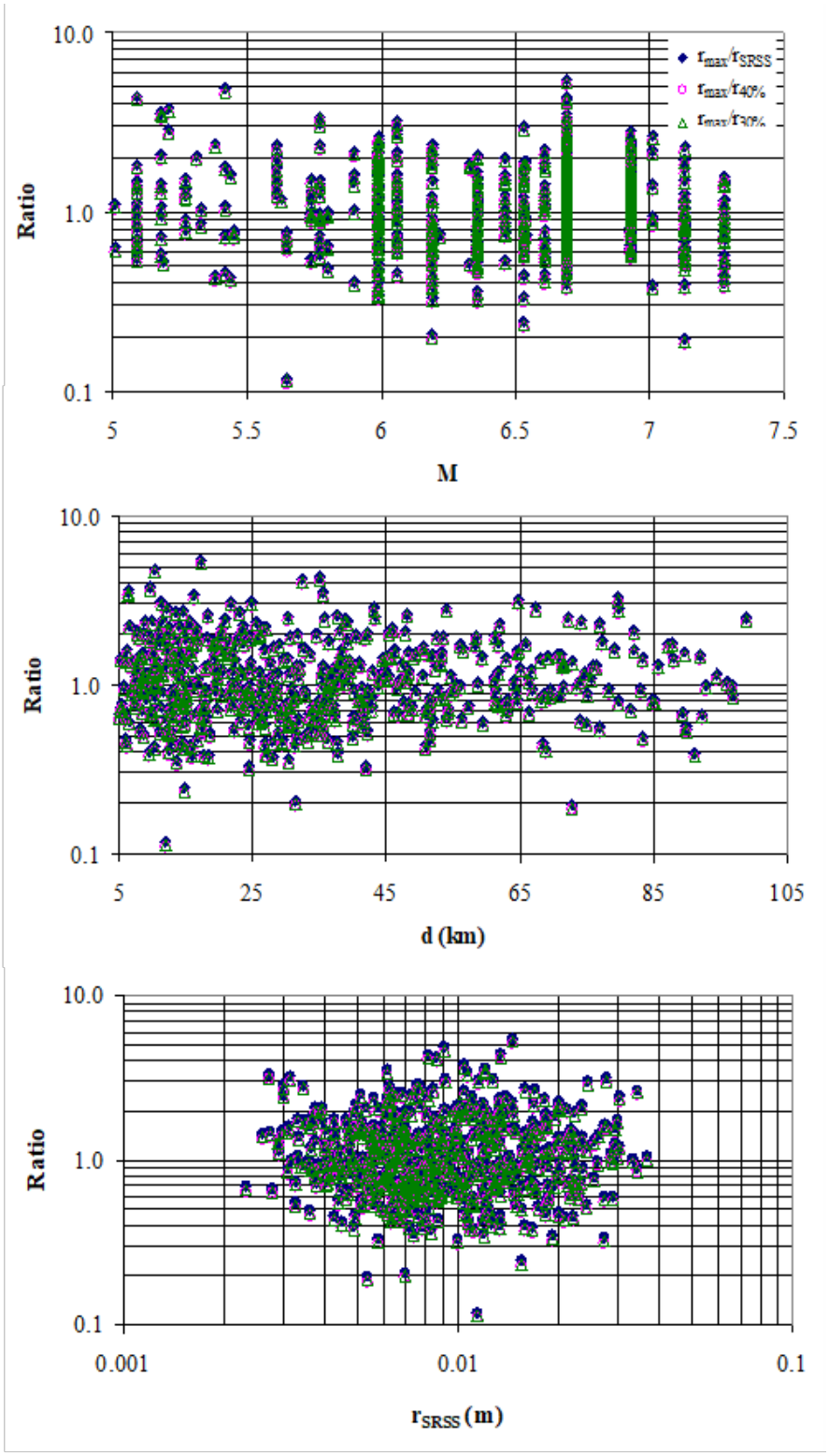

Figure 6. Ratios of r_{max}/r_{rule} versus the magnitude *M*, distance *d* and r_{srss}.

Table 4. Obtained parameters considering the SRSS rule and percentage rules and Eq. (9).

Structure characteristics			SRSS			40%-rule			30%-rule		
ζ_x	T_{nx}	η_y	a	$\sigma_{\eta e}$	$\sigma_{\eta r}$	a	$\sigma_{\eta e}$	$\sigma_{\eta r}$	a	$\sigma_{\eta e}$	$\sigma_{\eta r}$
3	0.2	1	-0.011	0.205	0.495	-0.084	0.205	0.495	-0.054	0.205	0.495
2	0.2	0.4	0.092	0.167	0.499	0.023	0.169	0.499	0.065	0.170	0.499
1	0.5	1	0.012	0.223	0.539	0.022	0.223	0.539	0.096	0.223	0.539
0.5	0.5	0.5	0.059	0.314	0.565	-0.007	0.313	0.565	0.018	0.313	0.565
1/3	1	1	0.030	0.322	0.582	-0.042	0.322	0.582	-0.013	0.322	0.582

By carrying out similar analysis for structures shown in Figure 5, the obtained model parameters are also listed in Table 4. Again, the results presented in the table indicate that $\sigma_{\eta e}$ and $\sigma_{\varepsilon r}$ are similar to $\sigma_{\varepsilon e}$ and $\sigma_{\eta r}$ shown in Table 1, and that the biases for the considered structures are is within about 10% for the SRSS rule, 8% for the 40% rule and 10% for the 30% rule. Therefore, the variability associated with the GMPE shown in Eq. (9) for estimating the structural responses under bidirectional excitations is similar to that of the GMPE (i.e., attenuation relation) for SDOF systems; and the former is only slightly biased while the latter is not biased. This bias depends on the structural characteristics, and one could correct this bias by increasing the estimated r_{rule} by about 10% for the SRSS rule and the 30% rule, and by increasing the estimated r_{rule} by about 8% for the 40% rule if the contributions to the overall responses by the vibration in one or the other direction are similar. The unconservatism in the SRSS rule may be attributed to the assumption that the excitations in two orthogonal horizontal directions are uncorrelated. Overall, for different combination rules the statistics are almost identical and the biases are surprisingly close. This indicates that the accuracies of the rules, on average, are very similar.

It is noteworthy that to appreciate the accuracy of the rules alone, one could use the PSA values obtained directly from each record rather than ones from the GMPEs in estimating the difference $\ln(r_{max})$-$\ln(r_{rule})$. In such cases, the mean of r_{max}/r_{rule} ranges from 0.99 and 1.04, and its standard deviation is always less than 0.27. However, since the combined use of the rules and the PSA values estimated from each record is deemed less unpractical, no further assessment of this ratio is reported in the following.

Since the PSA or the modal responses along the structural principal axes are considered to be the same in the above analysis, r_c given in Eq. (3) is statistically independent of the angle of seismic incidence. To discuss the critical response r_{cr} associated with the critical angle of incidence θ_{cr}, one must consider that the spectra differ for two orthogonal directions. However, the uniform hazard spectra and the design spectrum given in design codes are developed based on $A(T_n)$ for randomly oriented SDOF systems and do not represent the responses in two orthogonal directions. To overcome this and aimed at developing a simple representation of the response spectra for the two response axes or for the two principal directions, one could directly relate the response spectra for orthogonal horizontal direction to $A(T_n)$. The response spectra for the two response axes could be given in terms of $A_{MaxR}(T_n)$ and $A_{MinR}(T_n)$ which can be approximated by $1.30A(T_n)$, $0.70A(T_n)$ as shown Section 3 and Table 2; while the spectra for the two principal axes are given in terms of $A_{Pma}(T_n)$ and $A_{Pmi}(T_n)$ and can be approximated by $1.15A(T_n)$ and $0.95A(T_n)$. Based on these considerations, for a given structure one could calculate the samples of the ratio between the predicted critical response by the extended CQC rule to $r_{max,c}$ as follows:

1) Evaluate $r_{max,c}$ for the i-th record (with corresponding magnitude and distance denoted by $(M, d)i$).

2) Calculate critical response r_{cr} using the extended CQC rule shown in Eq. (3), and denote it by $r_{cr,m}$ if the spectra are defined by ($A_{MaxR}(T_n)$,

$A_{MinR}(T_n))=(1.30A(T_n),\ 0.70A(Tn))$ γ equals 0.54 (=0.7/1.3) and, by $r_{cr,p}$ if the spectra are defined by ($A_{P-ma}(T_n)$, $A_{Pmi}(T_n)$)=(1.15$A(T_n)$, 0.95$A(T_n)$) and γ equals 0.83 (=0.95/1.15). Note that $A(T_n)$ is predicted by Eq. (6) for $(M, d)_i$ with ε equal to zero.

3) Calculate the ratios $r_{max,m}/r_{cr,m}$ and $r_{max,m}/r_{cr,p}$ for the considered record.

By repeating these steps for all the considered records, samples of the ratios, which are obtained for the structures shown in Figure 4, are depicted in Figure 7. Figure 7 is used to illustrate possible linear correlation between the logarithmic of the ratios to the magnitude *M*, distance *d*, $\ln(r_{cr,m})$ and $\ln(r_{cr,p})$ for the structure considered in Figure 4. Again, the plot suggests that the logarithmic of the considered ratios could be assumed to be linearly uncorrelated with *M*, distance *d*, $\ln(r_{cr,m})$ and $\ln(r_{cr,p})$ since in all cases the correlation coefficients are less than about 0.10. Similar results to those shown in Figure 7 are obtained for the structures considered in Figure 5. However, no apparent differences can be observed, and for that reason they are not presented.

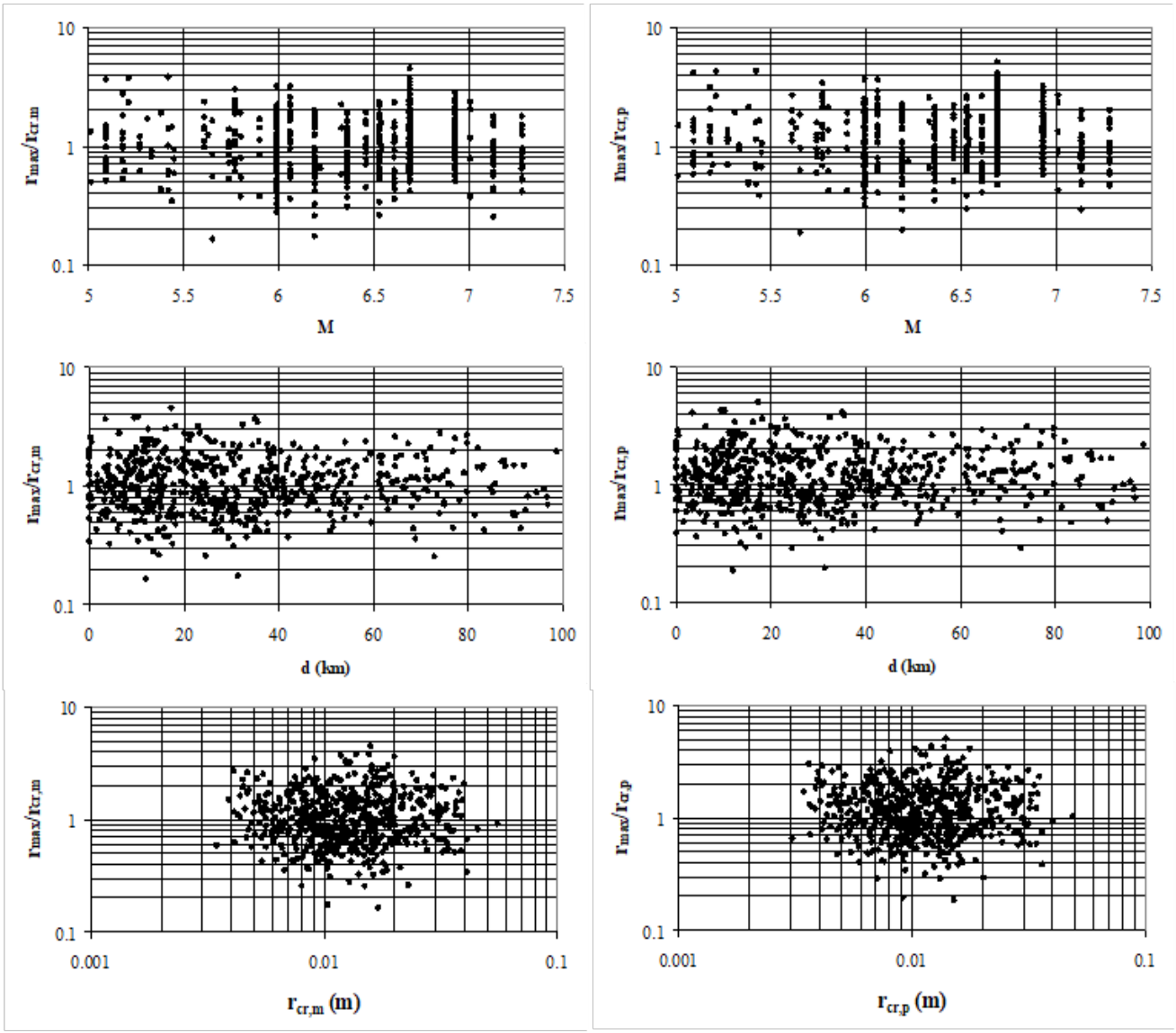

Figure 7.Samples of $r_{max,m}/r_{cr,m}$ and $r_{max,m}/r_{cr,p}$ versus the magnitude *M*, distance *d*, $r_{cr,m}$ and $r_{cr,p}$.

To assess the uncertainty associated with $\ln(r_{max,c}/r_{cr,m})$ and with $\ln(r_{max,c}/r_{cr,p})$, and possible bias, one again must take into account both the inter- and intra-event variability. Therefore, similar to the previous case shown in Eq. (9), one could carry out regression analysis to assess this variability by considering,

$$\ln\left(r_{\max,c}\right)=\ln\left(r_{cr,m}\right)+a_m+\eta_m \qquad (10a)$$

and,

$$\ln\left(r_{\max,c}\right)=\ln\left(r_{cr,p}\right)+a_p+\eta_p \qquad (10b)$$

where a_m is a model parameter to be determined through regression analysis, ηm equals $\eta_{me}+\eta_{mr}$ in which η_{me} represents the inter-event variability with zero mean and standard deviation $\sigma_{\eta me}$ and η_{mr} represent the intra-event variability with zero mean and standard deviation $\sigma_{\eta me}$, and a_m , η_p, η_{pe}, η_{pr}, $\sigma_{\eta pe}$ and $\sigma_{\eta pr}$ are defined similarly.

By carrying out the regression analysis, the obtained model parameters and the standard deviations are shown in Table 5. Note that since in all cases a_m is smaller than ap and closer to zero, the use of the $(A_{MaxR}(T_n), A_{MinR}(T_n))$ in defining the spectra in two horizontal orthogonal directions for estimating the critical response is less biased than that of $(A_{Pma}(T_n), A_{Pmi}(T_n))$. The standard deviations of the intra-event and inter-event variability for η_{me} and η_{mr} are similar to those for ε and for η. On average for all considered cases, the bias in the estimated $r_{max,c}$ can be correct by increasing the responses about less than 15% if $r_{cr,m}$ is used, and by increasing the response less than 25% if $r_{cr,p}$ is used.

It must be emphasized that statistics and biases associated with using the extended CQC rule together with $(A_{MaxR}(T_n), A_{MinR}(T_n))=(1.30A(T_n), 0.70A(T_n))$ or $(A_{Pma}(T_n), A_{Pmi}(T_n))=(1.15A(T_n), 0.95A(T_n))$ shown in Table 5 are for cases where the responses depend on the bidirectional excitations. The above-mentioned corrections should not be applied if a response depends only on unidirectional excitations. The corrections factors developed are only applicable to linear SDOF systems under bidirectional excitations. Although the study of inelastic responses of systems under bidirectional seismic excitations has been reported in the literature (Lee and Hong, 2010), the development of correction factors for nonlinear MDOF structures is a potential area for future work and is outside the scope of the present study.

5. CONCLUSIONS

It is emphasized that the uniform hazard spectra or the design spectra are developed based on the ground motion prediction equation (GMPE) (or attenuation relation) for the pseudospectral acceleration (PSA) $A(T_n)$ of randomly oriented SDOF systems. Such a PSA differ from the PSA along the principal directions and along the response axes.

Based on statistics of the peak responses obtained from time history analysis of structures under bidi-

Table 5. Model parameters and standard deviations for Eq. (10) determined through regression analysis.

Structure characteristics			PSA defined by $(A_{MaxR}(T_n), A_{MinR}(T_n))$			PSA defined by $(A_{MaxR}(T_n), A_{MinR}(T_n))$		
ζ_x	T_{nx}	η_v	a_m	$\sigma_{\eta me}$	$\sigma_{\eta mr}$	a_p	$\sigma_{\eta pe}$	$\sigma_{\eta pr}$
3	0.2	1	-0.025	0.204	0.481	0.097	0.204	0.481
2	0.2	0.4	0.141	0.198	0.483	0.220	0.194	0.483
1	0.5	1	0.054	0.218	0.522	0.146	0.211	0.526
0.5	0.5	0.5	0.068	0.308	0.562	0.176	0.307	0.562
1/3	1	1	0.020	0.324	0.573	0.143	0.324	0.573

rectional seismic excitations of 592 records and from the combinations rules, it is concluded that the square-root-of-sum-of-squares (SRSS) rule, the 40% rule and the 30% rule give biased but surprisingly similar estimates of peak responses. The bias depends on the structural characteristics, and may be correct using scaling factors. More specifically, it is concluded that:

1) The maximum response for structures under randomly oriented bidirectional orthogonal horizontal excitations, r_{max}, is, on average, about 81% of the critical response, $r_{max,c}$ (see Table 3).

2) If the structural response is sensitive to bidirectional excitations, as a conservative approximation, the (orientation independent) peak response under bidirectional seismic excitations can be approximated by using $1.10r_{SRSS}$, $1.08r_{40\%}$ and $1.10r_{30\%}$ where r_{SRSS}, $r_{40\%}$ and $r_{30\%}$ are the responses calculated by using the SRSS rule, the 40% rule and the 30% rule, respectively, in which $A(T_n)$ is used in defining the spectra in two orthogonal horizontal directions (see Table 4).

To estimate the critical response, $r_{max,c}$, (i.e., response corresponding to the critical angle of seismic incidence) by using the extended complete quadratic combination (CQC) rule, it is suggested that the response spectra for the two orthogonal horizontal directions can be defined using ($1.30A(T_n)$, $0.70A(T_n)$), which are based on the response spectra along the response axes. Use of these spectra rather than the ones based on the principal axes, which are ($1.15A(T_n)$, $0.95A(T_n)$), provides less biased estimate of the critical responses (see Table 5). It is noted that the correction factors are based on predefined GMPE, the use of other GMPE could have an impact on the accuracy and bias of the evaluated combination rules.

For responses depending significantly on bidirectional excitations it is suggested that:

1) As a conservative approximation, $r_{max,c}$ can be approximated by $1.15r_{cr,m}$, where $r_{cr,m}$ denotes the estimated critical response obtained using the extended CQC rule and the mean of $A(T_n)$ is used in defining the spectra ($1.30A(T_n)$, $0.70A(T_n)$).

2) The scaling factor of 1.15 and $r_{cr,m}$ in the above are to be replaced by 1.25 and $r_{cr,p}$, if the spectral in two horizontal directions are defined along the principal axes (i.e., ($1.15A(T_n)$, $0.95A(T_n)$).

It is believed that these recommendations should be considered when the combination rules and design spectra are used in estimating the peak responses or critical peak responses under bidirectional excitations. Further, it is noted that the structural system type (e.g., reinforced concrete, steel, masonry) might influence the applicability of the proposed correction factors. Lee and Hong (2010) studied simplified structural models under bidirectional seismic excitations with hysteretic behavior represented by the Bouc–Wen model with biaxial interaction. The use of the Bouc–Wen model to represent inelastic behavior of structural systems is advantageous as the model can incorporate strength/stiffness degradation and take into account different degrees of biaxial interaction. Although the study by Lee and Hong (2010) represented a step forward the in the study of inelastic responses of hysteretic systems under bidirectional seismic excitations, the impact of the employ of different structural typologies on the correction factors is still a potential area for future work.

ACKNOWLEDGEMENTS

The financial support of the National Autonomous University of Mexico (UNAM) and the Secretariat of Science, Humanities, Technology and Innovation (SECIHTI) of Mexico and the Natural Science and Engineering Research Council of Canada, is gratefully acknowledged.

REFERENCES

Abrahamson, N. A., and Silva, W.J. (1997). "Empirical response spectral attenuation relations for shallow crustal earthquakes," Seism. Res. Lett., 68, 94-127.

Adams, J., and Atkinson, G. (2003). "Development of Seismic Hazard Maps for the Proposed 2005 Edition of the National Building Code of Canada," Canadian Journal of Civil Engineering, Vol. 30: 255-271.

Anastassiadis, K., Avramidis, I.E., and Panetsos, P. (2002). "Concurrent design forces in structures under three-component orthotropic seismic excitation." Earthquake Spectra, 18, 1-17.

Arias, A. (1970). "A Measure of Earthquake Intensity", R.J. Hansen, ed. Seismic Design for Nuclear Power Plants, MIT Press, Cambridge, Massachusetts, pp. 438-483.

Arias, A. (1996). "Local directivity of strong ground motion", Proc. of 11th World Conference on Earthquake Eng., Acapulco, Mexico, paper No. 1240.

Atkinson, G.M., and Boore, D.M. (2006). "Earthquake Ground-Motion Prediction Equations for Eastern North America." Bull. Seism. Soc. Am. 96, 2181-2205.

Boore, D.M., Joyner, W.B., and Fumal, T. E. (1997). "Equations for estimating horizontal response spectra and peak acceleration from western North America." Seism. Res. Lett. 68, 128-153.

Boore, D.M., Watson-Lamprey, J., and Abrahamson, N.A. (2006). "Orientation-independent measures of ground motion." Bull. Seism. Soc. Am. 96, 1502-1511.

Boore, D.M., and Atkinson, G.M. (2006). "NGA empirical ground motion model for the average horizontal component of PGA, PGV and SA at spectral periods of 0.1, 0.2, 1, 2, and 3 seconds." Interim Report for USGS Review, 50 pp.

Campbell, K. W., and Bozorgnia, Y. (2003). "Updated near-source ground-motion (attenuation) relations for the horizontal and vertical components of peak ground acceleration and acceleration response spectra." Bull. Seism. Soc. Am. 93, 314-331.

Chopra, A.K. (1996). "Emilio Rosenblueth's selected results." Proc. of 11th World Conference on Earthquake Eng., Acapulco, Mexico, paper No. 2016.

Chopra, A.K. (2001). "Dynamics of structures: Theory and application to earthquake engineering." Prentice-Hall, Englewood Cliffs, New Jersey. 844 pp.

Der Kiureghian, A. (1981). "A response spectrum method for random vibration analysis of MDOF systems." Earthquake Engineering and Structural Dynamics, 9, 419-435.

Frankel, A., Mueller, C., Barnhard, T., Perkins, D., Leyendecker, E. V., Dickman, N., Hanson, S., and Hopper, M. (1996). "National seismic hazard maps" Open File 96-532, U.S. Department of the Interior, U.S. Geological Survey, Denver, CO.

Hong, H.P., and Wang, S.S. (2002). "Probabilistic analysis of peak response with uncertain PSD function." Earthquake Engineering and Structural Dynamics, 31, 1719-1733.

Hong, H.P., and Goda, K. (2007). "Orientation-Dependent Ground-Motion Measure for Seismic-Hazard Assessment." Bull. Seism. Soc. Am. 97(5), 1525-1538.

Joyner, W. B., and D. M. Boore (1993). Methods for regression analysis of strong-motion data, Bull. Seism. Soc. Am. 83, 469-487.

Kubo, T., and Penzien, J. (1979). "Analysis of three-dimensional strong ground motions along principal axes, San Fernando earthquake." Earthquake Engineering and Structural Dynamics, 7(3), 265-278.

Lopez, O.A., Chopra, A. K., and Hernandez, J.J. (2001). "Evaluation of combination rules for maximum response calculation in multicomponent seismic analysis." Earthquake Engineering and Structural Dynamics, 30, 1379-1398.

Lee, C. S., & Hong, H. P. (2010). Statistics of inelastic responses of hysteretic systems under bidirectional seismic excitations. Engineering Structures, 32(7), 2074–2086. https://doi.org/10.1016/j.engstruct.2010.03.005

Menun, C. and Der Kiureghian, A. (1998) "A Replacement for the 30%, 40%, and SRSS Rules for Multicomponent Seismic Analysis." Earthquake Spectra, 14(1), 153-163.

Menun, C. and Der Kiureghian, A. (2000). "Envelopes for seismic response vectors. I: Theory." Journal of Structural Engineering, ASCE, 126(4), 467-473.

Newmark, N.M. (1975). "Seismic design criteria for structures and facilities, Trans-Alaska pipeline system." Proceedings of the U.S. National Conference on EarthquakeEngineering. Earthquake Engineering Institute, 94-103.

PEER. (2006). "Next Generation Attenuation database." Pacific Earthquake Engineering Research Center, <http://peer.berkeley.edu/nga/index.html> (last accessed April 4th, 2006).

Penzien, J., and Watabe, M. (1975). "Characteristics of 3-Dimensional earthquake ground motions." Earthquake Engineering and Structural Dynamics, 3, 365-373.

Pozos-Estrada, A., Hong, H.P., and Gómez-Martinez, R. (2007). "Medicion Bidireccional de Componentes Ho-

rizontales del Movimiento del Terreno para Sismos de Subduccion." Proc., National Congress of Seismic Engineering, Mexican Society of Seismic Engineering, Ixtapa-Zihuatanejo, Mexico, paper I-10. (in spanish).

Rosemblueth, E., and Contreras, H. (1997). "Approximate Design for mult-icomponent Earthquakes." Journal of Engineering Mechanics Division, ASCE, 103, 895-911.

Smeby, W., and Der Kiureghian, A. (1985). "Modal combination rules for multi-component earthquake excitation." Earthquake Engineering and Structural Dynamics, 13, 1-12.

Steidl, J. H., and Lee, Y. (2000). "The SCEC Phase III strong-motion database." Bull. Seism. Soc. Am. 90, S113-S135.

Wang, S.S. and Hong, H.P. (2005). "Probabilistic Analysis of Peak Response to Non-stationary Seismic Excitation." Structural Engineering and Mechanics, 20(5), 527-542.

Wang, J., Burton, H. V., & Dai, K. (2021). Reliability-based assessment of percentage combination rules considering the collapse performance of special concentrically braced frames. Engineering Structures, 226, 111370. https://doi.org/10.1016/j.engstruct.2020.111370

Wang, W., Wang, J., Dai, K., Tesfamariam, S., & El Damatty, A. (2024). Probabilistic evaluation of combination rules that account for orthogonal seismic effects in torsionally irregular structural design. Structures, 66, 106855. https://doi.org/10.1016/j.istruc.2024.106855